Heinrich, I., Touchan, R., Dorado Liñán, I., Vos, H., Helle, G. (2013): Winter-to-spring temperature dynamics in Turkey derived from tree rings since AD 1125. - Climate Dynamics, 41, 7-8, 1685-1701

DOI: 10.1007/s00382-013-1702-3

Winter-to-spring temperature dynamics in Turkey derived from tree rings since AD1125

Ingo Heinrich[1]*, Ramzi Touchan[2], Isabel Dorado Liñán[1], Heinz Vos[3], Gerhard Helle[1]

[1] *Helmholtz Centre Potsdam, GFZ German Research Centre for Geosciences, Telegrafenberg, 14473 Potsdam, Germany*

[2] *Laboratory of Tree-Ring Research, University of Arizona, Tucson, USA*

[3] *Forschungszentrum Jülich, Institute for Chemistry and Dynamics of the Geosphere, Wilhelm-Johnen-Str., 52425 Jülich, Germany*

* Corresponding author:

Helmholtz Centre Potsdam, GFZ German Research Centre for Geosciences,

Climate Dynamics and Landscape Evolution, Telegrafenberg, 14473 Potsdam, Germany

Tel.: +49 331 288 1915; fax: +49 331 288 1302

E-mail address: heinrich@gfz-potsdam.de

Abstract

In the eastern Mediterranean in general and in Turkey in particular, temperature reconstructions based on tree rings have not been achieved so far. Furthermore, centennial-long chronologies of stable isotopes are generally also missing. Recent studies have identified the tree species *Juniperus excelsa* as one of the most promising tree species in Turkey for developing long climate sensitive stable carbon isotope chronologies because this species is long-living and thus has the ability to capture low-frequency climate signals. We were able to develop a statistically robust, precisely dated and annually resolved chronology back to AD1125. We proved that variability of $\delta^{13}C$ in tree rings of *J. excelsa* is mainly dependent on winter-to-spring temperatures (January to May). Low-frequency trends, which were associated with the medieval warm period and the little ice age, were identified in the winter-to-spring temperature reconstruction, however, the 20^{th} century warming trend found elsewhere could not be identified in our proxy record, nor was it found in the corresponding meteorological data used for our study. Comparisons with other northern-hemispherical proxy data showed that similar low-frequency signals are present until the beginning of the 20^{th} century when the other proxies derived from further north indicate a significant warming while the winter-to-spring temperature proxy from SW-Turkey does not. Correlation analyses including our temperature reconstruction and seven well-known climate indices suggest that various atmospheric oscillation patterns are capable of influencing the temperature variations in SW-Turkey.

Keywords: tree rings; Juniperus excelsa; temperature reconstruction; stable carbon isotopes; $\delta^{13}C$; climate indices

1 Introduction

The climate of the eastern Mediterranean is characterised by extremes of heat, highly variable precipitation, and limited water resources. These features are of great significance to the growing human populations and can play a role in the dynamics of regional demographic, socio-cultural, economic, and environmental changes of the area (Türkeş 1998). Therefore, understanding natural climate variability is of great importance as it will help to better predict its future variability, thus helping the societies affected to better adapt to the effects of climate change. Developing this understanding is difficult from the relatively short instrumental record available for the eastern Mediterranean region (Türkeş and Erlat 2003). Gassner et al. (1942) already remarked that for most parts of Turkey meteorological data were collected only since the late 1920s. Alternatively, natural archives such as tree rings and other proxy records can be used to capture information about climate variability on longer time scales. Tree rings are unique in their ability to provide high-resolution, absolutely dated climate signals for the study of palaeoclimatology (Hughes et al. 2010).

Stable carbon isotopes in tree rings are valuable sources for studies on climate reconstructions. The variability of isotope records from tree rings is closely dependent on the impact of environmental changes on plant physiological processes, mainly photosynthesis and transpiration. During the vegetation period signals from plant ecophysiological processes are integrated over time into the individual tree rings. The use of stable carbon isotopes from plant organic material as a palaeoclimate proxy is based on a model which considers the fractionation of the stable carbon isotopes during photosynthetic uptake of CO_2 in the leaves. The degree of fractionation depends on the rate of stomatal conductance and the rate of photosynthesis, which are influenced by a number of direct and indirect factors such as the environmental factors precipitation and temperature (e.g., McCarroll and Loader 2004).

So far only a few dendroclimatological studies have been conducted in Turkey (Gassner et al. 1942; Akkemik 2000, 2003; D'Arrigo and Cullen, 2001; Hughes et al. 2001; Touchan et al., 2003, 2005; Akkemik and Aras, 2005; Griggs et al. 2007; Sevgi and Akkemik 2007; Touchan et al. 2007; Akkemik et al. 2005, 2008; Köse et al. 2011). Gassner et al. (1942) identified winter and spring precipitation as the major growth limiting factor while temperature did not play an important role in central Turkey. Akkemik (2000) determined the relationship between tree rings of *Pinus pinea* from the Istanbul region and temperature and precipitation data. He found a significant positive correlation with summer precipitation and a weak positive correlation with spring temperature. D'Arrigo and Cullen (2001) reconstructed precipitation back to AD 1628 for central Turkey based on five tree-ring chronologies. The reconstruction showed some correspondences with the Euphrates River streamflow and the North Atlantic Oscillation. Akkemik (2003) carried out a calibration study focusing on tree rings of *Cedrus libani* at the northern boundary of its natural distribution in northern Turkey. The response functions analysis suggested positive correlation between ring widths and winter-to-spring temperature and spring-to-summer precipitation. A reconstruction of spring precipitation back to AD 1635 using oak tree rings in the western Black Sea region of Turkey corroborated historical records of droughts in Turkey (Akkemik et al. 2005). Touchan et al. (2003, 2007) developed May-to-June precipitation reconstructions for southwestern Turkey based on tree rings of Cedar, Juniper and two Pine species. The reconstructions showed clear evidence of multi-year to decadal variations in spring precipitation. Additional analyses of links between large-scale climatic variation and these climate reconstructions showed some relationships between extremes in spring precipitation and anomalous atmospheric circulation in the region. However, the relationships between major European-scale circulation patterns and the reconstructed May-to-June precipitation was insignificant which suggested that more local factors and processes have mainly been influencing tree-ring variability over the last centuries (Touchan et al. 2005). Akkemik and Aras (2005) studied tree rings of *Pinus nigra* and developed a reconstruction of summer precipitation for southern Central Turkey back to AD 1689. Although the authors could identify a significant negative correlation between the North Atlantic oscillation and instrumental precipitation data, the correlation was lower and non-significant between the reconstructed precipitation and NAO. Griggs et al. (2007) found that May-to-June precipitation is the primary limiting factor in annual tree-ring growth of oaks of northeastern Greece and northwestern Turkey. Making use of this relationship the authors calculated a regional reconstruction of May-to-June precipitation for AD 1089-1989. The mean May-to-June temperature was also shown to be a growth-limiting factor indicated by a significant negative correlation. In tree-ring reconstructions of spring-summer precipitation and streamflow for north-western Turkey, which both emphasize high-frequency variations, Akkemik et al. (2008) were able to identify common climatic extremes back to AD 1650 over much of the country. In a dendroecological study of *Pinus nigra* at different altitudes in Kazdaglari, NW Turkey, Sevgi and Akkemik (2007) showed varying and unclear correlations between tree rings and climate. Precipitation was often positively correlated with tree rings in summer and temperature was positively correlated with tree rings either in winter or in spring-to-summer depending on the altitude.

Recently, Köse et al. (2011) reconstructed May–June precipitation for western Turkey by means of tree rings of *Pinus nigra*. The reconstruction contained mostly short drought events with the longest consecutive dry period between 1925 and 1928. The comparison with historical data of agricultural famine years suggested a close relationship to such dry years as determined from the reconstruction. Hughes et al. (2001), making use of a large archaeological dataset, conducted an extreme year analysis of a multi-millennial master tree-ring chronology for the Aegean region consisting mainly of archaeological wooden objects. They showed that the so-called pointer years were associated with circulation anomalies responsible for precipitation-bearing systems influencing the region in springtime.

The review of the studies conducted in Turkey so far has shown that several tree species have been investigated for their climate responses. The tree-ring series of most species seem to correlate best with precipitation and to some extent with temperature. However, the tree-ring studies were always based on ring-width measurements and always resulted in reconstructions of precipitation and drought indices. Studies of tree-ring based temperature reconstructions and stable isotopes in tree rings are, to our knowledge, still lacking in Turkey.

The aim of this paper is to present a first multi-centennial stable carbon isotope chronology derived from tree rings of *Juniperus excelsa* M. Bieb. trees from a mountainous site near Antalya, Turkey. Since this is the first tree-ring isotope record from Turkey, its usefulness for further palaeoclimatology is evaluated. We analyze its response to climate and reconstruct the selected climate variable. Since stable isotope series do not have age trend problems such as ring width measurements (McCarroll and Loader 2004; Gagen et al. 2006; Treydte et al. 2006), statistical *a-priori* filtering will not be necessary and hence it can be expected that high- and low-frequency climate signals will be retrieved from the isotope record.

Moreover, the study investigates the spatial and temporal correlation patterns of the climate growth relationships in order to assess the stability, i.e., quality of this new climate reconstruction in Turkey. It also aims to examine possible climate trends found similarly in our and other reconstructions derived from already existing proxy records and to assess if extremely cold or hot years indicated by our record are corroborated by historical documentary data.

Finally, temporal correlations calculated between the new climate proxy and various climate indices established for geographical regions surrounding Turkey (e.g., NAO, MOI, NINO4, etc.) are presented to help understand the climate dynamics in Turkey. The eastern Mediterranean is influenced by some of the most relevant mechanisms acting upon the global climate system. It lies in a transitional zone between the arid zone of the subtropical high of North Africa and the temperate zone of central and northern Europe affected by westerly flows. Several studies (Conte et al. 1989; Kutiel and Maheras 1998; Kadioglu et al. 1999; Kutiel and Benaroch 2002; Kutiel et al. 2002; Xoplaki 2002; Kutiel and Türkeş 2005; Türkeş and Erlat 2008, 2009) examined the temperature regime over the Eastern Mediterranean basin and the relationship between temperature variations and circulation indices in order to identify those indices that have the strongest influence on the temperature variations. The Mediterranean climate seems to be influenced by the South Asian Monsoon in summer, the Siberian High Pressure System in winter, and the El Niño Southern Oscillation (ENSO) and the North Atlantic Oscillation (NAO) throughout the year (e.g., Corte-Real et al. 1995; Maheras et al. 2000; Ribera et al. 2000).

2 Materials and methods

2.1 Study site

The study site Jsibeli (36°36’N / 30°01’E) is located near Elmali in the Antalya district of southwest Turkey at an elevation of 1850 to 2020 m above sea level (Fig. 1). The site is situated on the southwest slopes of the Taurus Mountains, which divide the Mediterranean coastal region from the central Anatolian Plateau. Based on the classification by Türkeş (1998) and Türkeş et al. (2002) Turkey has four major rainfall regions. Jsibeli is situated in the Mediterranean climate region (MED) which is characterized by dry, hot summers and cool, rainy winters (Türkeş 1996; Türkeş et al. 2002). In the MED region, precipitation follows a strong seasonal pattern, with most of the precipitation occurring during the cold season and small amounts during summer. The total annual precipitation is approximately 750 mm and the wintertime is characterized by a water surplus while the warmer seasons by a water deficit. The summer dryness is often associated with large-scale regional climate that is controlled by both mid-latitude (more European climate) and North African-Asiatic tropical (*e.g.*, monsoon low) pressure systems (Türkeş and Erlat 2003). Due to the relatively high altitude (1850-2020m a.s.l.), the site is covered with snow from December-to-April (Türkeş et al. 2002). The mean annual temperature ranges from 10.1°C to 13.2°C. July is the warmest month, with an average temperature between 20.3°C and 25.9°C. January is the coldest month, with an average temperature ranging from –4.9°C to 5.9°C (Turkish General Directorate of Meteorology 2008).

The site at Jsibeli is a pure *Juniperus excelsa* open forest stand with trees several hundred years old. This type of forest can be regarded as remnant after the Beyşehir occupation clearance phase which took place between 1250BC to AD800. Before this period southwest Turkey had been covered by various species of the genera *Cedrus*, *Pinus*, *Abies*, *Juniperus* and deciduous *Quercus* but afterwards it was dominated by *Pinus* alone (Roberts 1998).

Pollen diagrams suggest a possible change in climate from a continental to a more "Atlantic" climate during the Beyşehir occupation (Bottema and Woldring 1990).

2.2 Chronology building

For further isotope analysis 15 increment cores of five living trees and seven stem discs of seven dead trees were chosen from an initial sample pool comprising 54 cores and 14 stem discs (Touchan et al. 2007). In general, isotopic analyses require fewer sample trees than studies of tree-ring widths to provide a representative average series for a site because the common signal strength among isotope series is higher (Leavitt and Long 1984; Gagen et al. 2004). The selection criteria for the samples were a high correlation with the mean ring-width site chronology, smallest possible numbers of missing rings, no tree-ring sequences with ring widths below 0.1 mm to ensure always enough sample material, no significant growth suppressions and releases and no scars, reaction wood or other wound reactions to increase the common signal.

All cores were sanded and visually cross-dated following dendrochronological procedures described by Fritts (1976), Schweingruber (1983) and Cook and Kairiukstis (1990). Ring widths were measured with an accuracy of 0.01 mm, using the linear table Lintab™ (Frank Rinn S.A., Heidelberg, Germany) and the TSAP-Win program (Rinn 2003). The accuracy of the cross-dating and measurements was verified using the computer program COFECHA (Holmes 1983).

The samples were analysed individually and with annual resolution for $\delta^{13}C$. Tree rings were split manually with a scalpel using a stereomicroscope, and the α-cellulose extracted following the chemical method based on the use of sodium hydroxide and sodium chlorite (Loader et al. 1997). Usually α-cellulose is extracted to concentrate on one chemical compound because the different components of wood have different isotopic values (Wilson and Grinsted 1977).

The $^{13}C/^{12}C$ isotope ratios were measured as CO_2 by combusting the α-cellulose samples in an elemental analyzer (Model NA 1500; Carlo Erba, Milan, Italy) coupled via an open split to an isotope ratio mass spectrometer (Micromass Optima, Ltd. Manchester, UK) operating in continuous flow mode. Sample replication resulted in a precision of better than ±0.1‰ for $\delta^{13}C$ values. The isotope ratios are given in the conventional delta (δ) notation, relative to the standard VPDB ($\delta^{13}C$). The samples were analysed individually instead of pooling (Treydte et al. 2001; Dorado Liñán et al. 2011).

2.3 Data analysis

The $\delta^{13}C$ tree-ring series are affected by the depletion in atmospheric $^{13}CO_2$ due to fossil fuel burning and deforestation since the industrialization (ca. AD1850). The resulting changes in the carbon isotope source value introduces a decreasing trend which is not related to tree-physiological response to climatic or environmental change and needs to be removed from the raw $\delta^{13}C$ tree-ring series. The most common way is to subtract annual changes in $\delta^{13}C$ of atmospheric CO_2, obtained from ice cores and direct measurements, from each tree-ring stable isotope value (Leuenberger et al. 1992; Elsig et al. 2009). We applied this atmospheric correction to the $\delta^{13}C$ series before any manipulation of the carbon isotope data started (McCarroll and Loader 2004; Leuenberger 2007), thereby guaranteeing that the source value was kept constant for the entire time period.

Long term changes of the atmospheric $\delta^{13}C$ source value affect all trees equally but trees may respond differently to changing CO_2 concentrations. However, the persistence and extent of possible plant physiological effects are still under debate. Despite experimental evidence showing that elevated CO_2 levels increase growth and ^{13}C discrimination in most plants, the isolation of a $\delta^{13}C$ signal consistent with anthropogenically induced rises in atmospheric CO_2 from the tree-ring record has shown mixed results (McCarroll et al. 2009; Beerling 1996; Jahren et al. 2008). While Voelker et al. (2006) indicate that the enhancement effects of elevated CO_2 on tree growth declines with age, Saurer et al. (2003) found evidence for a downward adjustment of photosynthesis and diminishing isotope effects under elevated CO_2 only after a few years. In a recent study Schubert and Jahren (2012) comprehensively review the state of the art concerning the effects of atmospheric CO_2 concentration on carbon isotope fractionation. They highlight the diversity and non-linearity of the tree physiological responses and therefore additional detrending methods such as the PIN correction, as recently proposed by McCarroll et al. (2009), were not adopted in the current study in order not to produce artificial trends.

After the correction of the stable carbon isotope measurements, individual series of $\delta^{13}C$ were z-transformed to ensure an equal contribution of each series to the final chronology. The z-transformed $\delta^{13}C$ were tested for significant autocorrelation. The $\delta^{13}C$ had a high first order partial autocorrelation (p = 0.85, t-stat = 26.75) and therefore prewhitening of the series was tested (Meko 1981), which however, was not found to improve the climate reconstructions. Thus, prewhitening was rejected in favour of not prewhitening to preserve low-frequency climatic signals in the series (Esper et al. 2003). The individual z-transformed $\delta^{13}C$ series were finally averaged into one mean site chronology $\delta^{13}C_{CorZ}$ reaching back to the year AD1022. The corrected and z-transformed series $\delta^{13}C_{CorZ}$ was used for further dendroclimatological investigations.

The Expressed Population Signal (EPS, Wigley et al. 1984) was computed to assess the common signal representativeness of the final chronology. Theoretically, the EPS ranges from 0.0 to 1.0, i.e. from no agreement to perfect agreement with the population chronology, but Wigley et al. (1984) give an EPS = 0.85 as a reasonable limit for the chronology to still be reliable.

2.4 Climate data

The most complete meteorological records closest to the study site are recorded at the meteorological stations Elmali (36°44′N, 29°55′E), Isparta (37°46' N, 30°33'E) and Afyon (38°45'N, 30°32'E) (Turkish General Directorate of Meteorology 2008). Monthly precipitation and temperature data from the three stations were obtained to develop a regional climate series representing the mountainous inland region of southwest Turkey. The three stations are located at similar elevations (Elmali 1113m asl, Isparta 997m asl and Afyon 1034m asl). The available temperature records range from 1959 to 2000 for Elmali and from 1949 to 2006 at the other two stations. The time span for the precipitation data ranges between 1961 and 2000 in Elmali and 1931 and 2006 at the other two stations. Given the various time spans of availability of the meteorological data, and in order to avoid depending on a single station, we applied the method of Jones and Hulme (1996) to average the precipitation and temperature records for each month since the climate data were not of the same length in order to develop a mean regional series. Monthly values for each station were standardized as z-scores relative to the 1959-2000 (temperature) and 1961-2000 (precipitation) common periods and averaged to calculate monthly z-scores for the regional average series. These monthly z-scores were converted to 'absolute' values using the average of the means and standard deviations of each of the original monthly series. The complete regional temperature and precipitation records extend from 1949-2006 (temperature) and 1931-2006 (precipitation).

Before relationships between climate and growth were examined we first checked the meteorological data for inhomogeneities that might interfere with the tree-ring calibration procedure using the techniques recommended by Mitchell et al. (1966). For the comparison between stations, monthly precipitation data were summed cumulatively. The totals for one station were then plotted as a function of the totals for the other station resulting in so-called double mass plots. Monthly temperature data of two stations were differenced and the result summed cumulatively. Only homogeneous meteorological data were then used for further analysis.

2.5 Climate response, calibration, verification and reconstruction

The influence of climate on the stable isotope series was investigated by computing simple linear correlations (r) with monthly climate variables using a period from January of the previous year to October of the current year. The dominant climatic factor controlling tree growth at Jsibeli was calibrated against the site $\delta^{13}C_{CorZ}$ tree-ring chronology. The climate record was split into two periods. The first period, 2006-1978, is used for calibration and the second one, 1977-1949, for the independent verification of the data. The ordinary least square method was applied to find the best regression model which was then used as the transfer function (Fritts 1976). The Pearson's correlation coefficient between instrumental and reconstructed values, the Reduction of Error and the Coefficient of Efficiency (RE and CE; Cook et al. 1994) were computed to estimate the ability of the $\delta^{13}C_{CorZ}$ data to predict the selected climate factors. The verified simple linear regression model was then used to reconstruct climate for the site. The 95% confidence intervals for the reconstruction were calculated according to Chou (1972).

3 Results and discussion

The mean tree-ring width chronology, which was used for the isotope analysis, consists of 12 trees and covers the period from 1022 to 2006. The mixture of core samples from living trees and cross sections from dead stumps and logs accounts for the smaller sample depth between 1980 and 2006 (Fig. 2D). The tree-ring width series display long-term trends (Fig. 2A) indicating age trends which would normally be detrended if the aim was to use ring width data to reconstruct climate (Touchan et al. 2003, 2007), however, in this study we concentrated on stable carbon isotopes only. Between 1022 and 1124 the $\delta^{13}C_{CorZ}$ series consist of less than five trees and the EPS drops below the critical value 0.85. Therefore, the series was terminated in 1125 due to the small sample size in the older section and low EPS values. The rbar/EPS statistics for the tree-ring width and the $\delta^{13}C_{CorZ}$ chronologies are 0.48/0.87 and 0.44/0.85 for the period 1125 to 2006, respectively. However, it needs to be mentioned that due to the small sample size of only 4 samples the EPS drops to 0.8 during the period 1992 to 2006. Although, the EPS temporarily is somewhat below the critical value of 0.85, the overall values indicate that the mean $\delta^{13}C_{CorZ}$ chronology is a robust estimate of annual changes in $\delta^{13}C$ and that it is suitable for further dendroclimatic research.

The raw $\delta^{13}C$ series shows a prominent decline from approximately 1900 due to the decrease of atmospheric $\delta^{13}C$ values (Fig. 2B), which has been removed by the correction (Fig. 2C) (Leuenberger et al. 1992; Elsig et al. 2009). The $\delta^{13}C_{CorZ}$ series exhibits relatively low values in the period 1125 to the late 15th century, followed by a steady increase until the early 18th century and a sharp decrease towards the late 18th century. After two peaks in the early and late 19th century, the record stays relatively stable on an average level to then decrease from the mid-1990s until 2006 (Fig. 2C).

The climate response plots present correlations between $\delta^{13}C_{CorZ}$ chronology and climate data (Fig. 3). The analysis includes monthly climate data of the current (J-D) and previous (j-d) year, as well as annual and selected seasonal climate data. The analysis shows significant negative correlations between $\delta^{13}C_{CorZ}$ and precipitation of July to September ($r=-0.36$; $P < 0.01$). Highly significant correlations are shown for $\delta^{13}C_{CorZ}$ and May, January-to-March and January-to-May temperatures ($r=-0.44$, $r=-0.42$ and $r=-0.52$; $P < 0.001$, respectively) (Fig. 3).

This leads us to the assumptions of a distinct winter-to-spring temperature signal and a weak but significant summer-to-autumn precipitation signal recorded in the isotope record. The negative correlations suggest that the lower the temperatures in January to May and the lower the precipitation in July to September, the higher the values of $\delta^{13}C_{CorZ}$. The negative correlation of the mean $\delta^{13}C_{CorZ}$ chronology with winter-to-spring temperatures indicates growth stress due to low temperatures which is not surprising for a site with trees growing at altitudes of 1850 to 2020 m above sea level. Basically, the discrimination of the stable carbon isotopes depends on the stomatal conductance and the rate of photosynthesis (Farquhar et al. 1982). In winter-to-spring at such high elevations the rate of photosynthesis seems to be affected mainly by low temperatures. Years with cold winter and spring temperatures are likely to affect growth in two ways. In cold winters during dormancy the cambium and the leaves may be damaged more than usual and the following recovery in spring may take longer. Similar results have been described for pine trees in Sweden and northeast Germany (Troeng and Linder 1982; von Lührte 1991). Low spring temperatures may further delay the photosynthesis or slow down the rate of photosynthesis which will have negative effects on the cambial activity. In contrast, the non-significant correlations between $\delta^{13}C_{CorZ}$ and winter-to-spring precipitation demonstrates that stable carbon isotopes are not such a good proxy for precipitation as has been demonstrated for tree-ring width (Touchan et al. 2007). It seems as if the site receives enough moisture in form of snow and rainfall during the cold season. However, other proxies such as stable oxygen isotopes may be able to reveal a stronger moisture signal. During the summer-to-autumn period, humidity levels in the soil and the air turn low, and hence fractionation is depending more on the stomatal conductance which seems to change throughout the season due to the increasing vapor pressure deficit. Since $\delta^{13}C_{CorZ}$ correlated best with the temperature data, the mean January-to-May temperatures were calibrated against $\delta^{13}C_{CorZ}$ in tree rings.

The regression analysis between $\delta^{13}C_{CorZ}$ and the January-to-May temperature for the entire period 1949 to 2006 determined the linear relationship $y = -1.1735x + 7.3414$. The correlation $r = 0.42$ ($P < 0.001$) is highly significant for the calibration period (1978-2006) and also for the verification period 1949 to 1977 ($r = 0.61$; $P < 0.001$), and 27% of the $\delta^{13}C_{CorZ}$ variation is explained by the January-to-May temperature data. The reduction of error (RE) and coefficient of efficiency (CE) were calculated (Tab. 1) to provide an indication of the robustness of the relationship between $\delta^{13}C_{CorZ}$ and the January-to-May temperature.

Although the values are not very high (RE = 0.29 / CE = 0.28) both values are positive. The theoretical limits for the RE and CE statistics range from 1 which indicates perfect agreement to minus infinity. A minus value indicates no agreement but any positive value can be considered as encouraging (Fritts 1976).

Observed and modelled temperature values show only a few differences during the calibration and verification periods. In the calibration period more differences are apparent but generally the model follows the course of the observed data (Fig. 4). Nevertheless, the statistics indicate that the reconstruction is of good quality and stable in time. Based on the established climate growth relationship we here present the reconstruction of January-to-May temperature (Fig. 5).

The temperature reconstruction exhibits multi-decadal to centennial variability with winter-to-spring temperatures mostly above average for the period 1125 and 1510. The medieval warm period (MWP) is reflected by temperatures being constantly above the average between the early 12th and mid-14th century. Then temperatures decrease until 1700 with only a short increase around 1625. The little ice age (LIA) heralds itself by low values in the temperature reconstruction with the beginning of a decreasing temperature trend in 1475, and the LIA finally is in full swing during the 17^{th} and 18^{th} centuries, as indicted by very low reconstructed temperatures. The first winter-to-spring temperature minimum in 1700 is followed by a short increase until approximately 1730 to then drop again to the second absolute low in 1750. These two minima together with a third in the mid-19th century are generally agreed on and have been found elsewhere (Grove 1988).

When compared to well-known activity events of the Sun (Solanki et al. 2004) our reconstruction confirms high temperatures for periods of high solar activity during the Medieval Warm Period and low temperatures during large parts of the Wolf (1300-1380), Spörer (1480-1550), Maunder (1645-1715) and Dalton Minima (1790-1820). The modern solar maximum since the 1950s is reflected by higher reconstructed temperatures but only since the 1990s.

3.1 Comparison with documentary data

Comparing climate reconstructions based on proxies with historical documentary data often confirms that extremely narrow or wide rings were caused by severe climate conditions which not only had a significant impact on tree growth but at the same time had detrimental effects on the societies affected. Documentary data usually record extreme events such as very cold or prolonged drought periods (Hammer-Purgstall 1834-1836; Panzac 1985; Brázdil et al. 2005; Telelis 2005, 2008). Since documentary records from the Eastern Mediterranean mainly report extreme drought or flooding events (Kuniholm 1990), only a small number of written records regarding extreme temperature deviations can be found in the literature. Telelis (2005, 2008) analysed historical information from the time of the Byzantine Empire and grouped his results into cold, hot, wet and dry episodes. In the mediterranean to temperate semi-arid climate regions (Csa and BSk, respectively), Telelis (2005, 2008) identified the years 1230-1300, 1320-1400 and 1430-1450 as periods with a higher frequency of cold episodes, that is, with more than two cold events of long duration per decade. All three cold periods are also indicated by our reconstruction, however, extremely hot years were not identified neither by our data nor by the historical records. Kuniholm (1990) reviewed several historical records and found mainly hints to dry and hot summers. The only mention of cold temperatures is for the winter of 1611 to 1612 which must have been exceptionally rich in snow because notes were made for awful snow in Anatolia and that the French consul in Turkey was killed when heavy snow broke through his house. In our record the winter of 1611 to 1612 is only indicated as slightly below average, however, heavy snow does not necessarily mean low temperatures. The German traveller Naumann (1893) reported that the years 1873 and 1874 had devastating effects on the Turkish society. A very dry and hot summer 1873 followed by very cold winter 1873 to 1874 killed 150000 people and 100000 head of livestock. In our record the January-to-May temperature of 1874 is also one of the lowest since 1125 thereby corroborating the historical records.

3.2 Temperature trends

Remarkably, our winter-to-spring temperature reconstruction does not follow the 20th century warming trend, found elsewhere (Wahl et al. 2010). In fact, for most of the 20th century we have reconstructed relatively low winter-to-spring temperatures and our reconstruction suggests that temperatures are only increasing since the 1980s.

The temperature trends in our reconstruction are in line with trend analysis results of meteorological data from Turkey and other parts of the eastern Mediterranean. Based on the analyses of 85 individual station data in Turkey (Türkeş et al. 1995; Kadıoglu 1997), general decreasing trends in annual and seasonal mean surface air temperature series over much of Turkey were found. In particular, the coastal regions of Turkey were largely characterized by colder than long-term average temperature conditions during the period between the late 1960s and early 1990s. Nevertheless, this trend has begun to change recently in Turkey, particularly due to increases in the mean temperature of the spring and summer seasons (Türkeş et al. 2002). In the eastern Mediterranean, several studies dealing with long-term variations and trends of surface air temperatures have been conducted. In Greece, Proedrou et al. (1997) detected an overall cooling trend for the majority of Greek stations in winter for the entire period of 1951-93. Ben-Gai et al. (1999) analysed the maximum and minimum temperatures of 40 stations in Israel for the period 1964-94. They revealed that both temperatures were characterized by a significant decreasing trend during the cool season and by an increasing trend during the warm season. Feidas et al. (2004) found a cooling trend in winter temperatures in Greece for the period 1955-2001, whereas, summer showed an overall warming trend, however, neither was statistically significant. As a result, the overall trend of the annual values was nearly zero. Similar conclusions can be drawn from a global analysis by Schönwiese (2008) which indicates a weak decreasing trend of annual mean temperatures for Turkey in contrast to the overall increasing trend for large parts of Eurasia during the last 100 years. Xoplaki (2002) and Luterbacher et al. (2004) also found stable or temporarily decreasing temperatures for the Mediterranean in general and Turkey in particular.

Since previous analyses of meteorological data especially from the eastern Mediterranean have indicated diverging trends regarding winter and summer temperatures, the meteorological temperature data used during our reconstruction procedure were tested for possible trends. The test was the basic linear regression-based model in which time t (in years) was taken as the independent variable and temperature as the dependent variable. Under the usual regression assumptions a two-tailed t-test was conducted where the null hypothesis states that the slope coefficient is equal to 0. If this is true, then there is no linear relationship between the explanatory and dependent variables, i.e., no trend can be identified (Bahrenberg et al. 1990). Similar to the findings by Türkeş et al. (2002), the climate data used for the current study also revealed long-term trends between 1950 and 2006 (Fig. 6).

While in spring and autumn no obvious trends are visible, positive and negative trends in summer and winter, respectively, are noticeable. The slope parameter estimates are all positive, except for winter, however, the t-test statistics are only significant for summer. The trend analysis of meteorological data has identified similar seasonal trends as in Greece and Israel where increasing summer temperatures and decreasing winter temperatures have also been found (Proedrou et al. 1997; Ben-Gai et al. 1999; Feidas et al. 2004).

Since the existing studies and the trend analysis of the climate data suggest that dissimilar seasonal temperature trends are present at several locations not only in Turkey but in other Mediterranean countries as well, the 20th century temperature rise missing in our reconstruction cannot be regarded as an analysis artefact but seems to be a rather special feature of the climate in parts of Turkey and surrounding countries of the Mediterranean.

3.3 Comparison with other temperature reconstructions

The review of existing literature brought to light that no local temperature reconstructions based on tree rings are available from the Eastern Mediterranean. Due to this lack of material for direct comparison, our Turkish temperature reconstruction was compared to a collection of 92 regional, hemispherical and global temperature reconstructions (Wahl et al. 2010). Wahl et al. (2010) describe a newly integrated archive of high-resolution temperature reconstructions for the last 2000 years included in NOAA's National Climatic Data Center, from small regional to global scale. The 92 surface temperature records including global, hemispheric, regional, and local single time series reconstructions were downloaded from the PaleoClimate Network (PCN v. 2.0.0) at http://www.ncdc.noaa.gov/paleo/pubs/pcn/pcn.html. Most of the records reconstruct annual mean temperatures with annual resolution for the last Millennium (Wahl et al. 2010). The reconstructions were compared with our Turkish reconstruction by means of simple Pearson´s correlation analysis and those correlating best with it were selected for further examination.

The correlation analysis revealed that many of the records do not correlate well with our Turkish reconstruction. Several reasons may be held responsible: many of the records are less suitable because they are local or regional reconstructions far away from Turkey, they are reconstructions for other seasons and the reconstructions are shorter or have a lower resolution.

From the 92 reconstructions those of Moberg et al. (2005) and Mann et al. (2008) were selected for further examination because they correlated best over the entire common period of 881 years. The correlation was more specified by comparing high-, band-, and low-pass filtered versions of the series (Fig. 7). The filtering was achieved by calculating the 11- and 61-year centred moving averages of the individual series which was followed by a decomposition of the original data into the three different components. The correlation patterns, separated into the three different frequency domains, revealed that the two hemispherical temperature reconstructions agree with our Turkish reconstruction only in the low frequency indicated by highly significant correlations.

When plotted together it is obvious that the three temperature reconstructions share common long-term trends (Fig. 8). All three records show above average temperatures during the medieval period and also some similar decadal-scale variations. They also contain a long-term descent to an all-time low at around 1700 and then temperatures start to increase again, however, the Turkish reconstruction does not follow the temperature rise indicated by the two hemispherical reconstructions during the 20th century.

In other frequency domains no strong correlations were identified which may be explained by the fact that most of the records used for the two hemispherical temperature reconstructions were derived from proxies located much further to the north. Temperature proxies from the north such as the European Alps, Scandinavia or Russia may be too far away from our Turkish reconstruction to contain the same high-frequency signals because the limiting factors of tree growth are too site-specific and differ too much inter-annually. Furthermore, the hemispherical records are annual mean temperatures while our Turkish reconstruction is a January-to-May temperature proxy.

3.4 Spatial correlation and spectral analysis

While the correlations with other temperature proxies were high only in the low-frequency domain, in a next step it was also interesting to spatially correlate our $\delta^{13}C_{CorZ}$ record with gridded winter-to-spring temperature data, in order to identify the geographic regions with significant correlations between temperature and our $\delta^{13}C_{CorZ}$ record. We used the KNMI Climate Explorer website (http://www.knmi.nl/) (van Oldenborgh and Burgers 2005) to generate correlation fields with seasonal January-to-May temperatures.

The spatial field correlations indicate that our $\delta^{13}C_{CorZ}$ record does not correlate with any January-to-May temperature grids in Northern or Central Europe during the analysis period

2006 to 1949 (Fig. 9). However, the map demonstrates that, intriguingly, most of the field correlation is oriented towards the south and east of the study site, that is, the spatial correlation between the $\delta^{13}C_{CorZ}$ chronology and the January-to-May mean temperature covers an area of most of Turkey, Syria and northeast Africa.

From this spatial analysis the question may arise what is actually influencing temperature variations in Turkey. The graphical oscillation patterns of the reconstructed January-to-May mean temperature and its 61-year moving average (Fig. 5 and 8) already suggests the presence of some low-frequency variability.

For further analysis of such possible non-random variations our temperature reconstruction was subjected to a spectral analysis to decompose it into different frequencies and analyse the variance in each frequency band to uncover possible trends and periodicities (Jenkins and Watts 1968). The software package Autosignal (Systat) determines those spectral density values that appear particularly strong and enables an easy graphical estimation of possible trends within the chronology (Davis 1986). The spectral analysis plot investigates possible reoccurring cycles (Fig. 10). Significant peaks at approximately 26, 32, 40, 55 and 87 years can be identified. Such multi-decadal peaks fall into the bandwidths of various climate indices such as the North Atlantic Oscillation (NAO), Arctic Oscillation (AO) or Mediterranean Oscillation (MO). Since some of the spectral peaks are similar to those known from prominent climate indices, we decided to compare our temperature reconstruction with a selection of such climate indices to identify likely candidates for having an influence on the reconstructed winter-to-spring temperatures in SW-Turkey.

3.5 Comparison of temperature reconstruction with circulation indices

The North Atlantic Oscillation (NAO) is the most important large scale mode of climate variability in the Northern Hemisphere. The NAO describes a large scale meridional fluctuation of atmospheric masses between the North Atlantic regions of the subtropical anticyclone near the Azores and the subpolar low pressure system near Iceland. The North Atlantic Oscillation (NAO) has been shown to be connected to the interannual variability of climatic conditions in the Mediterranean (Hurrel 1996; Werner and Schönwiese 2002).

The Arctic Oscillation (AO) is a teleconnection pattern characterized by a seesaw of atmospheric pressure between the Arctic and northern middle latitudes (Thompson and Wallace 1998). When the AO index (AOI) is positive, changes in the circulation patterns bring cooler and drier conditions to the Mediterranean basin. The negative phase is characterized by warmer and wetter conditions in the Mediterranean. Some studies have shown that the AO is closely connected to the interannual variability of mid- to high-latitude climates (e.g., Wang et al. 2005).

Conte et al. (1989) suggested the existence of the so-called Mediterranean Oscillation (MO) which reflects a dipole or seesaw effect between Alger and Cairo mean annual geopotential heights at the 500 hPa level. Based on this concept, a dipole-behaviour of the temperatures between the western and eastern Mediterranean have been attributed to the MO (Kutiel and Maheras 1998; Maheras and Kutiel 1999). Favourable conditions for high temperatures in one part are associated with unfavourable conditions in the other part and *vice versa*.

Kutiel and Benaroch (2002) identified a new seesaw feature they named the North Sea-Caspian Pattern (NCP). They defined the NCP as an upper level atmospheric teleconnection between the North Sea and the northern Caspian. The North Sea-Caspian Pattern Index (NCPI) is negative most of the year. Negative NCPI episodes are more frequent than positive, but during the 1990s there has been an increase in positive NCPI episodes.

The East Atlantic/West Russia (EAWR) pattern is a prominent teleconnection pattern that affects Eurasia throughout the year (Barnston and Livezey 1987). During the negative (positive) EAWR phases, wetter (drier) than normal weather conditions are observed over a large part of the Mediterranean (Krichak and Alpert 2005).

The El Nino Southern Oscillation (ENSO) is a climate pattern that occurs across the tropical Pacific Ocean. The term El Niño (La Niña) refers to warming (cooling) of the central and eastern tropical Pacific Ocean which leads to a major shift in weather patterns every three to eight years across the Pacific. ENSO is the oscillation between El Niño and La Niña conditions (Allan et al. 1996).

The Indian Ocean Dipole Mode Index (DMI), as defined by Saji et al. (1999), is an indicator of the east-west sea surface temperature (SST) gradient across the tropical Indian Ocean, linked to the Indian Ocean dipole mode, a zonal mode of the interannual variability of the Indian Ocean. A positive (negative) DMI is defined as above (below) normal SST in the tropical western Indian Ocean and below (above) normal SST in the tropical eastern Indian Ocean (Saji et al. 1999). Associated with a positive DMI phase are surplus Indian summer monsoon rainfall and an intensified upward motion of air over India. The associated divergent flow in the upper troposphere progresses westward and converges over the Mediterranean where the decent of air is intensified, constructing a zonal-vertical circulation cell from the northern India towards the Mediterranean region (Guan and Yamagata 2003).

Since all the above climate indices have the potential to influence the temperature variation in Turkey, monthly and seasonally averaged indices of the indices were correlated with our Turkish January-to-May temperature reconstruction (Tab. 2). Since the indices MOI, NCPI and EAWR reach back only to the 1950s, all correlations were computed for the period 1950 to 2006 maximising their comparability with the other indices.

The correlations for NAO and AO are negative for May-to-June of the previous year and March-to-May of the current year, and the strongest correlation is indicated between the January-to-May temperature reconstruction and the AOI of May-to-June of the previous year. Xoplaki (2002) also showed negative correlations between NAO and temperatures in winter for the Eastern Mediterranean. Statistically significant negative relationships between winter temperatures and the winter NAO Index were discovered in Israel (Ben-Gai et al. 2001), in

Egypt (Hasanean 2004), Greece (Feidas et al. 2004) and Turkey (Türkeş and Erlat 2009). Wang et al. (2005) revealed that negative AO phases correspond to warm conditions in Turkey and the Middle East. Xoplaki (2002) showed that the influence of the negative winter AO on the Mediterranean climate was generally towards warmer and drier conditions over the southern and eastern parts of the Mediterranean region including Turkey. Türkeş and Erlat (2008) revealed significant negative correlations between the variability of winter mean temperatures in Turkey and the AO.

The correlation between our temperature reconstruction and the MOI was negative but low for most of the months. We only identified a significant negative correlation in August of the previous year. In comparison, in the eastern Mediterranean a negative correlation between the MOI and winter temperature has been found (Feidas et al. 2004), i.e., when the MOI was in a positive (negative) phase, temperatures in the eastern Mediterranean were below (above) average. The relationship between NCPI and the January-to-May temperature reconstruction is characterized by positive correlations in July and October of the previous year and negative correlations in April to May of the previous year and February to April of the current year. Kutiel and Türkes (2005) also found negative correlations which meant that negative NCPI episodes tended to cause above normal temperatures in Turkey. In a comprehensive comparison, Türkeş and Erlat (2009) demonstrated that the NCPI and the AO are more capable than the NAO for explaining the year-to-year temperature variability in Turkey. The correlation between the EAWR index and the January-to-May temperature reconstruction is positive in June and negative in August, both months of the previous year. Over the eastern Mediterranean region positive (negative) EAWR winter periods are associated with more (less) intense northern air flows (Krichak et al. 2002), which result in below (above) average temperature conditions in the eastern Mediterranean.

Significant positive correlations resulted from the comparison between the January-to-May temperature reconstruction and NINO4 and DMI. Positive correlations are illustrated for May, June and August of the previous year. Similarly, in the Eastern Mediterranean there is some evidence that El Niño events are positively correlated with winter rainfall (Kadioglu et al. 1999). On the other hand, Pozo-Vázquez et al. (2005) found a non-linear response to ENSO in the Eastern Mediterranean. Negative precipitation anomalies with similar amplitude anomalies occurred both during El Niño and La Niña events. During El Niño events meridional shifts of the jet stream have been observed in the Eastern Mediterranean (Alpert et al. 2006). Other relationships between Eastern Mediterranean weather conditions and ENSO have been suggested, but these are generally weak or not stable (Xoplaki 2002). The strongest descent of the Indian Ocean dipole mode (DMI) circulation pattern, which has also been coined monsoon-desert mechanism (Rodwell and Hoskins 1996), is centered over the eastern Mediterranean, covering southeastern Europe and the eastern Sahara desert, where it is likely to inhibit convection and to cause dry or arid conditions (Saji and Yamagata 2003).

The climate indices NINO4 and DMI are mainly associated with climatic influences coming from the southeast and they are positively correlated with the January-to-May temperature reconstruction. In comparison, positive phases of the two indices seem to result in higher January-to-May temperatures while positive phases of all the other indices seem to cause below-average temperatures in winter to spring.

Furthermore, the analysis illustrates that our temperature reconstruction is more correlated to the climate index values of the previous year than of the current, although for two indices, that is, AO and NCPI, significant correlations are also shown for February-to-May of the current year. This suggests an often delayed reaction of the trees to changes of the climate indices. However, the climate indices themselves do not alter tree growth directly but the indices indicate changing climate conditions responsible for tree growth alterations. It seems likely that changing indices in the middle of the previous year indicate climate shifts which impact on tree growth, delayed by several months, in the next year.

The fact that various climate indices seem to have significant effects on the reconstructed temperature variations suggests that the climate at the study site in Southwest Turkey is affected by a mixture of climate mechanisms which are responsible for the temperature variations limiting Juniper tree growth in SW Turkey. At least two reasons can be proposed that may explain the mixture of correlations with all indices. The first is that some of the indices also correlate with each other since they describe similar or related oscillation patterns, such as the NAO, AO and NCPI. The second reason is that the correlation between the temperature and the indices is unstable in time which would indicate that in some years the temperature variations in Southwest Turkey are more influenced by one index while in the following years they are more affected by others as has been identified similarly in Australia (Heinrich et al. 2009).

For a more detailed analysis of this second scenario of different influences, correlations between the January-to-May temperature reconstruction and January-to-May averages of the climate indices were calculated in moving windows of 13 years (Heinrich et al. 2009). We found varying correlations in time between the reconstruction and indices (due to different lengths of the indices separated into Figs. 11 and 12). This result explains the limited correlations between our reconstruction and the indices when analysing them for the entire period. The correlations of the shorter series with our temperature reconstruction suggest significant values for the EAWR only between 1975 and 1990 (Fig. 11). The correlations between our reconstruction and the MOI and the EAWR, respectively, run mostly in opposite direction which indicates that temperature variations in some years are more influenced by Mediterranean atmospheric oscillation patterns and in other years by the East Atlantic West Russia pattern.

The correlations of the longer series with our temperature reconstruction also give some insights into the temporal dynamics of the relationships. The similar correlations between our reconstruction, NAO and AO, respectively, suggest that both climate indices represent related atmospheric oscillation patterns which have comparable influences on the temperature variations in Southwest Turkey. The correlation between our temperature reconstruction and NAO and AO runs in opposite direction to the correlation between the reconstruction and the DMI (Fig. 12). The same holds true for the correlations of the reconstruction with the DMI and NINO4, respectively. While in some years the climate in Turkey seems to be influenced by varying atmospheric conditions coming from the West to Northwest indicated by good correlations with NAO and AO, in other years it is influenced more by Southeastern atmospheric oscillation patterns suggested by good correlations with DMI and NINO4. The results substantiate expectations for the climate in Turkey situated in a transitional zone between the temperate zone of central and northern Europe affected by westerly flows, the arid zone of the subtropical high of North Africa and in the periphery of the monsoonal system acting in the Southeast. Overall, such correlation patterns changing synchronously imply that the climate in Southwest Turkey is influenced by various atmospheric oscillation patterns as has previously been indicated for the Eastern Mediterranean by Feidas et al. (2004), Xoplaki (2002) and Luterbacher et al. (2004).

4 Conclusions

We have presented the first precisely dated and climatically sensitive stable carbon isotope tree-ring chronology for Turkey where heretofore there were no such tree-ring proxies available. The $\delta^{13}C_{CorZ}$ mean chronology showed significant negative correlations with summer precipitation and January-to-May temperatures, which lead us to the assumptions of a distinct winter-to-spring temperature signal and a weak but significant summer-to-autumn precipitation signal recorded in the isotope record. Since results of previous studies from the eastern Mediterranean indicated temporally changing temperature trends which also differed seasonally and between the countries, our new reconstruction is interesting in particular regarding its long-term behaviour. In the absence of any other high resolution temperature proxy from Turkey our new temperature reconstruction is a valuable addition to the regional proxy data in the eastern Mediterranean. Low-frequency variations, which were associated with the medieval warm period and the little ice age, were identified in the winter-to-spring temperature reconstruction, however, the 20th century warming trend found elsewhere could not be identified in our temperature proxy record. The analysis of the corresponding meteorological data used for our study and results of temperature trend analyses conducted previously by others in the Eastern Mediterranean corroborated our result that the winter-to-spring temperatures in the region have not increased during the 20th century. Comparisons with other proxy data from the Northern Hemisphere showed that similar low-frequency signals can be identified until the beginning of the 20th century when other proxies derived from further north indicate a significant warming. The spatial correlation patterns demonstrated strong links between our $\delta^{13}C_{CorZ}$ chronology and the January-to-May mean temperatures from the Eastern Mediterranean and northeast Africa but no links to northern and central Europe. The temperature reconstruction revealed multi-decadal oscillations ranging between 87 and 26 years which are in the frequency range of some prominent atmospheric oscillation patterns such as NAO. The variety of oscillations contained by the $\delta^{13}C_{CorZ}$ chronology suggests that the atmospheric oscillation patterns are capable of influencing the temperature variations in Southwest Turkey. Correlation analyses including our temperature reconstruction and seven well-known climate indices which represent atmospheric oscillation patterns possibly impacting the study region illustrated temporally and geographically changing links between our reconstruction and the oscillation patterns. In some instances the correlations ran in opposite directions which implied complex relationships between the climate patterns. A multi-proxy approach comprising chronologies of tree-ring width, stable isotopes, wood density and quantitative wood anatomy measurements seems indispensable to better understand the long-term climate dynamics in the

Eastern Mediterranean, particularly in Turkey where so far only tree-ring width series have been used as high-resolution proxies.

Acknowledgements

We thank Carmen Bürger and Christoph Küppers for their help in the laboratory. This research was funded by the EU project MILLENNIUM (#017008).

References

Akkemik Ü (2000) Dendroclimatology of umbrella pine (*Pinus pinea* L.) in Istanbul (Turkey). Tree-ring Bull 56:17–20

Akkemik Ü (2003) Tree rings of *Cedrus libani* at the northern boundary of its natural distribution. IAWA J 24:63–73

Akkemik Ü, Aras A (2005) Reconstruction (1689–1994) of April-August precipitation in southwestern part of central Turkey. Int J Climatol 25:537–548

Akkemik Ü, Dagdeviren N, Aras A (2005) A preliminary reconstruction (A.D. 1635–2000) of spring precipitation using oak tree rings in the western Black Sea region of Turkey. Int J Biomet 49:297–302. doi:10.1007/s00484-004-0249-8

Akkemik Ü, D'Arrigo R, Cherubini P, Köse N, Jacoby GC (2008) Tree-ring reconstructions of precipitation and streamflow for north-western Turkey. Int J Climatol 28:173–183

Allan R, Lindesay J, Parker D (1996) El Niño southern oscillation and climatic variability. CSIRO Publishing, Collingwood, Australia

Alpert P, Baldi M, Ilani R, Krichak S, Price C, Rodó X, Saaroni H, Ziv B, Kishcha P, Barkan J, Mariotti A, Xoplaki E (2006) Relations between climate variability in the Mediterranean region and the tropics: ENSO, South Asian and African monsoons, hurricanes and Saharan dust. In: Lionello P, Malanotte-Rizzoli P, Boscolo R (eds) Mediterranean Climate Variability. Elsevier, Amsterdam, pp 149–177

Bahrenberg G, Giese E, Nipper J (1990) Statistische Methoden in der Geographie. Bd. 1 Univariate und bivariate Statistik. Teubner, Stuttgart

Barnston A G, Livezey RE (1987) Classification, seasonality and persistence of low-frequency atmospheric circulation patterns. Mon Wea Rev 115:1083–1126

Ben-Gai T, Bitan A, Manes A, Alpert P, Rubin S (1999) Temporal and spatial trends of temperature patterns in Israel. Theor Appl Climatol 64:163–177

Ben-Gai T, Bitan A, Manes A, Alpert P, Kushnir Y (2001) Temperature and surface pressure anomalies in Israel and the North Atlantic Oscillation. Theor Appl Climatol 69:171–177

Beerling D J (1996) ^{13}C discrimination by fossil leaves during the late-glacial climate oscillation 12–10 ka BP: measurements and physiological controls. Oecologia 108:29–37

Bottema S, Woldring H (1990) Anthropogenic indicators in the pollen record of the Eastern Mediterranean. In: Bottema S, Entjes-Nieborg G, van Zeist W (eds) Man's role in the shaping of the eastern Mediterranean landscape. Balkema, Rotterdam, pp 231–64

Brázdil R, Pfister C, Wanner H, von Storch H, Luterbacher J (2005) Historical climatology in Europe - the state of the art. Clim Change 70:363–430

Chou Y (1972) Probability and statistics for decision making. Holt, Rinehart, Winston, NY

Conte M, Giuffrida S, Tedesco S (1989) The Mediterranean oscillation: impact on precipitation and hydrology in Italy. In: Proceedings of the Conference on Climate and Water 1. Publications of Academy of Finland, Helsinki, pp 121–137

Cook ER, Kairiukstis LA (1990) Methods of Dendrochronology. Kluver, Dordrecht, Netherlands

Cook ER, Briffa KR, Jones PD (1994) Spatial regression methods in dendroclimatology: A review and comparison of two techniques. Int J Climatol 14:379–402

Corte-Real J, Zhang X, Wang X (1995) Large-scale circulation regimes and surface climatic anomalies over the Mediterranean. Int J Climatol 15:1135–1150

D’Arrigo R, Cullen HM (2001) A 350-year (AD 1628–1980) reconstruction of Turkish precipitation. Dendrochronologia 19:169–177

Davis JC (1986) Statistics and data analysis in Geology. 2nd Edition. John Wiley & Sons, New York

Dorado Liñán I, Gutierrez E, Helle G, Heinrich I, Andreu-Hayles L, Plannels O, Leuenberger M, Bürger C, Schleser G (2011) Pooled versus separate measurements of tree-ring stable isotopes. Sci Total Environ 409:2244–2251

Elsig J, Schmitt J, Leuenberger D, Schneider R, Eyer M, Leuenberger M, Joos F, Fischer H, Stocker TF (2009) Stable isotope constraints on Holocene carbon cycle changes from an Antarctic ice core. Nature 461:507–510. doi:10.1038/nature08393

Esper J, Cook ER, Krusic PJ, Peters K, Schweingruber FH (2003) Tests of the RCS method for preserving low-frequency variability in long tree-ring chronologies. Tree-Ring Res 59:81–98

Farquhar GD, O'Leary MH, Berry JA (1982) On the relationship between carbon isotope discrimination and the intercellular carbon dioxide concentration in leaves. Aust J Plant Physiol 9:121–137

Feidas H, Makrogiannis T, Bora-Senta F (2004) Trend analysis of air temperature time series in Greece and their relationship with circulation using surface and satellite data: 1955–2001. Theor Appl Climatol 79:185–208

Fritts HC (1976) Tree Rings and Climate. Blackburn Press, Caldwell, NJ

Gagen M, McCarroll D, Edouard J-L (2004) Latewood width, maximum density, and stable carbon isotope ratios of pine as climate indicators in a dry subalpine environment, French Alps. Arct Antarct Alp Res 36:166–171

Gagen M, McCarroll D, Edouard J-L (2006) Combining tree ring width, density and stable carbon isotope series to enhance the climate signal in tree rings: an example from the French Alps. Clim Change 78:363–379

Gassner G, Christiansen-Weniger F (1942) Dendroklimatologische Untersuchungen über die Jahresringentwicklung der Kiefern in Anatolien. Nova Acta Leopold 12:1-137

Griggs CB, Degaetano AT, Kuniholm PI, Newton MW (2007) A regional reconstruction of May-June precipitation in the north Aegean from oak tree-rings, AD 1089-1989. Int J Climatol 27, 1075–1089

Grove JM (1988) The Little Ice Age. Methuen, London

Guan Z, Yamagata T (2003) The unusual summer of 1994 in East Asia: IOD Teleconnections. Geophys Res Lett. doi:10.1029/2002GL016831

von Hammer-Purgstall J (1834-1836) Geschichte des osmanischen Reiches. Pesth, Hartleben

Hasanean HM (2004) Wintertime surface temperature in Egypt in relation to the associated atmospheric circulation. Int J Climatol 24:985–999. doi:10.1002/joc.1043

Heinrich I, Weidner K, Helle G, Vos H, Lindesay J, Banks JCG (2009) Interdecadal modulation of the relationship between ENSO, IPO and precipitation: insights from tree rings in Australia. Climate Dyn 33: 63–73. doi:10.1007/s00382-009-0544-5

Holmes RL (1994) Dendrochronolgy Program Manual. Laboratory of Tree-ring Research. Tucson, Arizona

Hughes MK, Kuniholm PI, Garfin GM, Latini C, Eischeid J (2001) Aegean tree-ring signature years explained. Tree-ring Research 57:67–73

Hughes MK, Swetnam TW, Diaz HF (2010) Dendroclimatology: Developments in Paleoenvironmental Research

Hurrell JW (1996) Influence of variations in extratropical wintertime teleconnections on Northern Hemisphere temperature. Geophys Res Lett 23:665–668

Jahren AH, Arens NC, Harbeson SA (2008) Prediction of atmospheric $\delta^{13}CO_2$ using fossil plant tissues. Rev Geophys 46:1–12

Jenkins GM, Watts DG (1968) Spectral analysis and its applications. Holden-Day, San Francisco

Jones PD, Hulme M (1996) Calculating regional climatic time series for temperature and precipitation: methods and illustrations. Int J Climatol 16:361–377

Kadıoğlu M (1997) Trends in surface air temperature data over Turkey. Int J Climatol 17:511–520

Kadıoğlu M, Tulunay Y, Borhan Y (1999) Variability of Turkish precipitation compared to El Nino events. Geophys Res Lett 26:1597–1600

Köse N, Akkemik Ü, Dalfes HN, Özeren MS (2011): Tree-ring reconstructions of May-June precipitation for western Anatolia. Quat Res 75:438–450. doi:10.1016/j.yqres.2010.12.005

Krichak SO, Kishcha P, Alpert P (2002) Decadal trends of main Eurasian oscillations and the Mediterranean precipitation. Theor Appl Climatol 72:209–220

Krichak SO, Alpert P (2005) Decadal trends in the east Atlantic–west Russia pattern and Mediterranean precipitation. Int J Climatol 25:183–192. doi:10.1002/joc.1124

Kuniholm PE (1990) Archaeological evidence and non-evidence for climatic change. In: Runcorn SJ, Peckers J-C (eds) The Earth's climate and variability of the sun over recent millennia. Philosophical Transactions of the Royal Society of London A, pp 645-655

Kutiel H, Maheras P (1998) Variations in the temperature regime across the Mediterranean during the last century and their relationship with circulation indices. Theor Appl Climatol 61:39–53

Kutiel H, Benaroch Y (2002) North Sea-Caspian Pattern (NCP)-An upper level atmospheric teleconnection affecting the Eastern Mediterranean: Identification and definitions. Theor Appl Climatol 71:17–28

Kutiel H, Maheras P, Türkeş M, Paz S (2002) North Sea – Caspian Pattern (NCP) – an upper level atmospheric teleconnection affecting the eastern Mediterranean – implications on the regional climate. Theor Appl Climatol 72:173–192

Kutiel H, Türkeş M (2005) New evidence about the role of the North Sea – Caspian Pattern (NCP) on the temperature and precipitation regimes in continental central Turkey. Geogr Ann A 87:501–513

Leavitt SW, Long A (1984) Sampling strategy for stable carbon isotope analysis of tree rings in pine. Nature 301:145–147

Leuenberger M (2007) To what extent can ice core data contribute to the understanding of plant ecological developments of the past? In: Dawson T, Siegwolf R (eds) Stable Isotopes as Indicators of Ecological Change. Academic Press, London, pp 211–234

Leuenberger M, Siegenthaler U, Langway CC (1992) Carbon isotope composition of atmospheric CO_2 during the last ice-age from an Antarctic ice core. Nature 357:488–490

Loader NJ, Robertson I, Barker AC, Switsur VR, Waterhouse JS (1997) An improved technique for the batch processing of small wholewood samples to α-cellulose. Chem Geol 136:313–317

Luterbacher J, Dietrich D, Xoplaki E, Grosjean M, Wanner H (2004) European seasonal and annual temperature variability, trends, and extremes since 1500. Science 303:1499–1503

Maheras P, Kutiel H (1999) Spatial and temporal variations in the temperature regime in the Mediterranean and their relationship with circulation during the last century. Int J Climatol 19:745–764

Maheras P, Patrikas I, Karacostas T, Anagnostopoulou C (2000) Automatic classification of circulation types in Greece: methodology, description, frequency, variability and trend analysis. Theor Appl Climatol 67:205–223

Mann ME, Zhang Z, Hughes MK, Bradley RS, Miller SK, Rutherford S, Ni F (2008) Proxy-based reconstructions of hemispheric and global surface temperature variations over the past two millennia. Proc Nat Acad Sci USA 105:13252–13257

McCarroll D, Loader NJ (2004) Stable isotopes in tree rings. Quaternary Sci Revi 23:771–801

McCarroll D, Gagen MH, Loader NJ, Robertson I, Anchukaitis KJ, Los S, Young GHF, Jalkanen R, Kirchhefer AJ, Waterhouse JS (2009) Correction of tree ring stable carbon isotope chronologies for changes in the carbon dioxide content of the atmosphere. Geochim Cosmochim Ac 73:1539–1547

Meko DM (1981) Applications of Box-Jenkins Methods of time-series analysis to reconstruction of drought from tree rings, Ph.D. Dissertation, University of Arizona, Tucson, pp 149

Mitchell JM Jr, Dzerdzeevskii B, Flohn H, Hofmeyr WL, Lamb HH, Rao KN, Wallen CC (1966) Climate change. Report of a working group of the Commission for Climatology, World Meteorological Organization Technical Note 79, Geneva

Moberg A, Sonechkin DM, Holmgren K, Datsenko NM, Karlén W (2005) Highly variable Northern Hemisphere Temperatures Reconstructed from Low- and High-Resolution Proxy Data. Nature 433:613–617

Naumann C (1893) Vom Goldenen Horn zu den Quellen des Euphrat: Munich, Leipzig

Panzac D (1985) La Peste Dans l’empire Ottoman 1700-1850. Editions Peeters, Louvain

Pozo-Vázquez D, Gámiz-Fortis SR, Tovar-Pescador J, Esteban-Parra MJ, Castro-Díez Y (2005) El Niño–Southern Oscillation events and associated European winter precipitation anomalies. Int J Climatol 25:17–31

Proedrou M, Theoharatos G, Cartalis C (1997) Variations and trends in annual and seasonal air temperature in Greece determined from the ground and satellite measurements. Theor Appl Climatol 57:65–78

Ribera P, Garcia R, Diaz HF, Gimeno L, Hernandez E (2000) Trends and interannual oscillations in the main sea-level surface pressure patterns over the Mediterranean 1955–1990, Geophys Res Lett 27:1143–1146. doi:10.1029/1999GL010899

Rinn (2003) TSAP-Win: Time Series Analysis and Presentation for Dendrochronology and Related Applications. Frank Rinn, Heidelberg, Germany

Roberts N (1998) The Holocene: an environmental history. Blackwell, Oxford

Rodwell MJ, Hoskins BJ (1996) Monsoons and the dynamics of deserts. Q J Roy Meteor Soc 122:1385–1404

Saji NH, Goswami BN, Vinayachandran PN, Yamagata T (1999) A dipole mode in the tropical Indian Ocean. Nature 401:360–363

Saji, N.H. and T. Yamagata (2003): Possible impacts of Indian Ocean Dipole mode events on global climate. Climate Res 25:151–169

Saurer M, Cherubini P, Bonani G, Siegwolf R (2003) Tracing carbon uptake from a natural CO_2 spring into tree rings: an isotope approach. Tree Physiol 23:997–1004

Schönwiese CD (2008) Klimatologie. Ulmer, Stuttgart

Schubert BA, Jahren AH (2012) The effect of atmospheric CO_2 concentration on carbon isotope fractionation in C_3 land plants. Geochimica et Cosmochimica Acta 96:29-43

Schweingruber FH (1983) Der Jahrring. Standort, Methodik, Zeit und Klima in der Dendrochronologie. Paul Haupt, Bern

Sevgi O, Akkemik Ü (2007) A Dendroecological study on Pinus nigra Arn. on the different altitudes of northern slopes of Kazdagları, Turkey. Indian J Environ Biol 28:73–75

Solanki SK, Usoskin IG, Kromer B, Schüssler M, Beer J (2004) An unusually active Sun during recent decades compared to the previous 11,000 years. Nature 431:1084–1087

Telelis IG (2005) Historical-climatological information from the time of the Byzantine Empire (4th - 15th centuries AD). Hist Meteor 2:41–50

Telelis IG (2008) Climatic fluctuations in the Eastern Mediterranean and the Middle East AD 300-1500 from Byzantine documentary and proxy physical palaeoclimatic evidence - a comparison. Jahrb Österr Byzantinistik 58:167–207

Thompson DWJ, Wallace JM (1998) The Artic Oscillation signature in the wintertime geopotential height and temperature fields. Geophys Res Lett 25:1297–1300

Touchan R, Garfin GM, Meko DM, Funkhouser G, Erkan N, Hughes MK, Wallin BS (2003) Preliminary reconstructions of spring precipitation in southwestern Turkey from tree-ring width. Int J Climatol 23:157–171

Touchan R, Xoplaki E, Funkhouser G, Luterbacher J, Hughes MK, Erkan N, Akkemik U, Stephan J (2005) Reconstruction of spring/summer precipitation for the Eastern Mediterranean from tree ring widths and its connection to large-scale atmospheric circulation. Climate Dyn 25:75–98

Touchan R, Akkemik Ü, Hughes MK, Erkan N (2007) May-June precipitation reconstruction of southwestern Anatolia, Turkey during the last 900 years from tree rings. Quaternary Res 68:196–202

Treydte K, Schleser GH, Schweingruber FH, Winiger M (2001) The climatic significance of $\delta^{13}C$ in subalpine spruces (Lötschental, Swiss Alps) - a case study with respect to altitude, exposure and soil moisture. Tellus 53:593–611

Treydte K, Schleser GH, Helle G, Frank DC, Winiger M, Haug, GH, Esper J (2006) The twentieth century was the wettest period in northern Pakistan over the past millennium. Nature 440:1179–1182

Troeng E, Linder S (1982) Gas exchange in a 20-year-old stand of Scots pine. Physiol Plantarum 54:7–23

Türkeş M (1996) Spatial and temporal analysis of annual rainfall variations in Turkey. Int J Climatol 16:1057–1076

Türkeş M (1998) Influence of geopotential heights, cyclone frequency and Southern Oscillation on rainfall variations in Turkey. Int J Climatol 18:649–680

Türkeş M, Sümer U, Kiliç G (1995) Variations and trends in annual mean air temperatures in Turkey with respect to climatic variability. Int J Climatol 15:557–569

Türkeş M, Sümer UM, Kiliç G (2002) Persistence and periodicity in the precipitation series of Turkey and associations with 500 hPa geopotential heights. Climate Res 21:59–81

Türkeş M, Sümer UM, Demir I (2002) Re-evaluation of trends and changes in mean, maximum and minimum temperatures of Turkey for the period 1929-1999. Int J Climatol 22:947–977

Türkeş M, Erlat E (2003) Precipitation changes and variability in Turkey linked to the North Atlantic oscillation during the period 1930-2000. Int J Climatol 23:1771–1796

Türkeş M, Erlat E (2008) Influence of the Arctic Oscillation on variability of winter mean temperatures in Turkey. Theor Appl Climatol 92:75–85. doi:10.1007/s00704-007-0310-8

Türkeş M, Erlat E (2009) Winter mean temperature variability in Turkey associated with the North Atlantic Oscillation. Meteorol Atmos Phys 105:211–225. doi:10.1007/s00703-009-0046-3

Turkish General Directorate of Meteorology (2008) Weather Station Databanks of Turkish General Directorate of Meteorology, Ankara

van Oldenborgh GJ, Burgers G (2005) Searching for decadal variations in ENSO precipitation teleconnections. Geophys Res Lett 32:L15701. doi:10.1029/2005GL023110

Voelker SL, Muzika R-M, Guyette, RP, Stambaugh MC (2006) Historical CO_2 growth enhancement declines with age in *Quercus* and *Pinus*. Ecol Monogr 76:549–564

von Lürthe A (1991) Dendroökologische Untersuchungen an Kiefern und Eichen in den stadtnahen Berliner Forsten. Landschaftsentwicklung und Umweltforschung. Schriftenreihe des Fachbereichs Landschaftsentwicklung der TU Berlin 77, pp 186

Wahl ER, Anderson DM, Bauer BA, Buckner R, Gille EP, Gross WS, Hartman M, Shah A (2010) An archive of high-resolution temperature reconstructions over the past 2+ millennia. Geochem Geophys Geosyst 11:Q01001. doi:10.1029/2009GC002817

Wang D, Wang C, Yang X, Lu J (2005) Winter Northern Hemisphere surface air temperature variability associated with the Arctic Oscillation and North Atlantic Oscillation. Geophys Res Lett 32:L16706. doi:10.1029/2005GL022952

Werner A, Schönwiese C-D (2002) A statistical analysis of the North Atlantic Oscillation and its impact on European temperature. Global Atmosph Osc System 8:293–306

Wigley TML, Briffa K, Jones PD (1984) On the average value of correlated time series, with applications in dendroclimatology and hydrometeorology. J Clim Appl Meteorol 23:201–213

Wilson AT, Grinsted MJ (1977) 12C/13C in cellulose and lignin as palaeothermometers. Nature 265:133–135

Xoplaki E (2002) Climate variability over the Mediterranean. Ph.D. thesis, University of Bern, pp 193

List of Figures and Tables

Fig. 1 Map with location of the sample site Jsibeli and climate diagram for the regional climate series representing the mountainous inland region of SW Turkey, period 1949-2006 for temperature and 1931-2006 for precipitation. The three stations, indicated by triangles, are located at similar elevations (Elmali 1113m asl, Isparta 997m asl and Afyon 1034m asl (Turkish General Directorate of Meteorology 2008).

Fig. 2 Plots of the Jsibeli raw tree-ring width series (A), raw $\delta^{13}C$ series (B), $\delta^{13}C$ corrected and z-transformed series ($\delta^{13}C_{CorZ)}$ (C) and sample depth for A to C (D) through time. The red graphs represent the means of the raw and the corrected series.

Fig. 3 Climate response plot for the Jsibeli site with the regional climate series (meteorological data from Elmali, Isparta and Afyon): monthly coefficients of correlation for mean temperatures (black bars) and precipitation sums (grey bars), significance levels are 0.05 (*), 0.01 (**), and 0.001 (***). Small letters on the left half of the diagram cover the period January to December of the previous year and capital letters represent January to December of the current year. Small letters a to d stand for annual values (current year) and the periods January-to-March, January-to-May and July-to-September of the current season, respectively.

Fig. 4 Reconstructed (solid line) and observed January-to-May temperature (dashed line) for calibration period 1978 to 2006 and verification period 1949 to 1977.

Fig. 5 Reconstruction of January-to-May temperature based on $\delta^{13}C_{CorZ}$ with 95% confidence intervals (CI calculated according to Chou 1972).

Fig. 6 Comparison of trends in seasonal temperature data of composite record Elmali, Isparta and Afyon (Winter: blue, Spring: green, Summer: red, Autumn: brown).

Fig. 7 Correlations (1125-2006) between the Turkish January-to-May temperature reconstruction and two hemispherical temperature reconstructions; high-, band-, and low-pass filtered (A, B, C) versions of Mann et al. 2008 (always left) and Moberg et al. 2005 (always right), significance levels are 0.05 (*), 0.01 (**), and 0.001 (***).

Fig. 8 Comparison of the Turkish January-to-May temperature reconstruction and two hemispherical temperature reconstructions (Mann et al. 2008, brown, and Moberg et al. 2005, green), 61-year moving averages.

Fig. 9 Spatial field correlations (van Oldenborgh and Burgers, 2005) between mean Jan-May temperature and $\delta^{13}C_{CorZ}$ (1949-2006), upper map: old world overview, lower map: eastern Mediterranean, black star indicates location of the study site .

Fig. 10 Spectral analysis of the Jan-May temperature reconstruction for the period 1125-2006 shows significant peaks at approximately 87, 54, 40, 32 and 26 years. 50, 90, 95, 99 and 99.9 % confidence levels are indicated.

Fig. 11 Coefficients of correlation between Jan-May temperature reconstruction and Jan-May MOI (red), NCPI (blue) and EAWR (green) in moving windows of 13 years (95 % confidence levels are indicated); for comparison printed on top, the z-scores of the corresponding series (MOI red, NCPI blue, EAWR green and Jan-May temperature reconstruction in black, all smoothed with a 13-year mean).

Fig. 12 Coefficients of correlation between Jan-May temperature reconstruction and Jan-May NAO (red), AO (blue), NINO4 (brown) and DMI (orange) in moving windows of 13 years (95 % confidence levels are indicated); for comparison printed on top, the z-scores of the corresponding series (NAO red, AO blue, NINO4 brown, DMI orange and Jan-May temperature reconstruction in black, all smoothed with a 13-year mean).

Table 1 Reconstruction statistics for $\delta^{13}C_{CorZ}$

Table 2 Comparison of correlations between the Jan-May temperature reconstruction and monthly to seasonal climate indices (NAO, AO, MOI, NCPI, EAWR, NINO4 and DMI) (small letters: months of previous year; capital letters: months of current year; confidence levels: 95%=bolt; 99%=bolt & underlined; 99.9%= bolt, underlined & italics; the confidence intervals differ slightly due to selected time series lengths; 56 yrs: NAO, AO, EAWR, NINO4; 50 yrs: MOI, DMI; 40 yrs: NCPI)

Figures and Tables

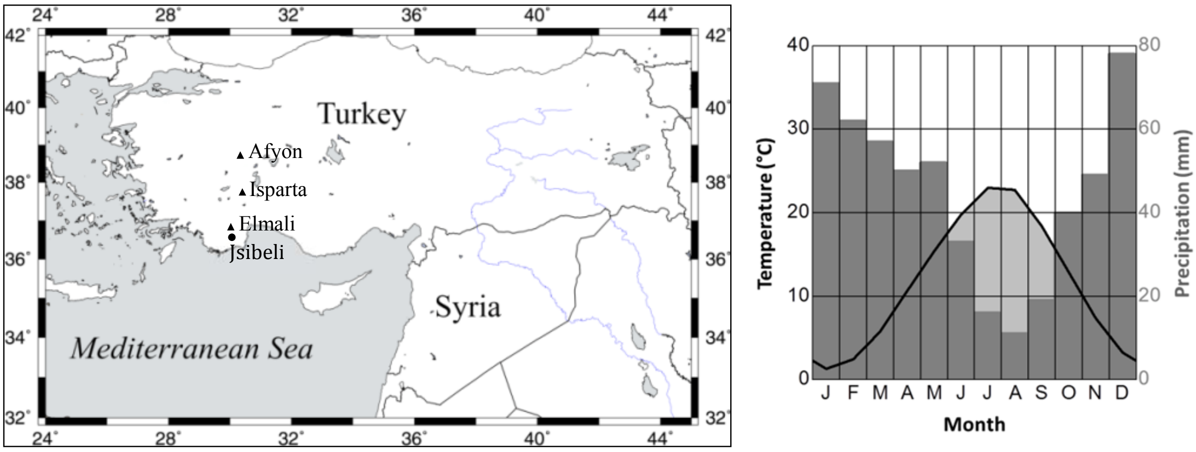

Fig. 1 Map with location of the sample site Jsibeli and climate diagram for the regional climate series representing the mountainous inland region of SW Turkey, period 1949-2006 for temperature and 1931-2006 for precipitation. The three stations, indicated by triangles, are located at similar elevations (Elmali 1113m asl, Isparta 997m asl and Afyon 1034m asl (Turkish General Directorate of Meteorology 2008).

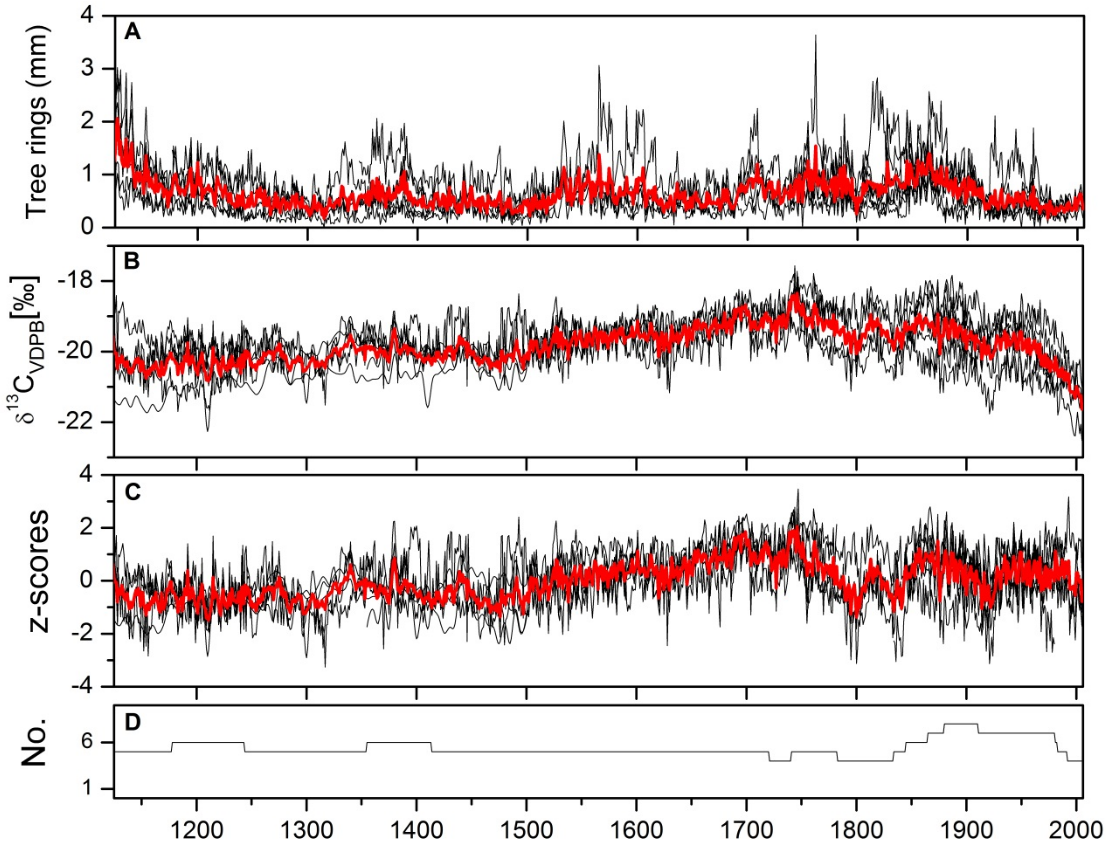

Fig. 2 Plots of the Jsibeli raw tree-ring width series (A), raw $\delta^{13}C$ series (B), $\delta^{13}C$ corrected and z-transformed series ($\delta^{13}C_{CorZ}$) (C) and sample depth for A to C (D) through time. The red graphs represent the means of the raw and the corrected series.

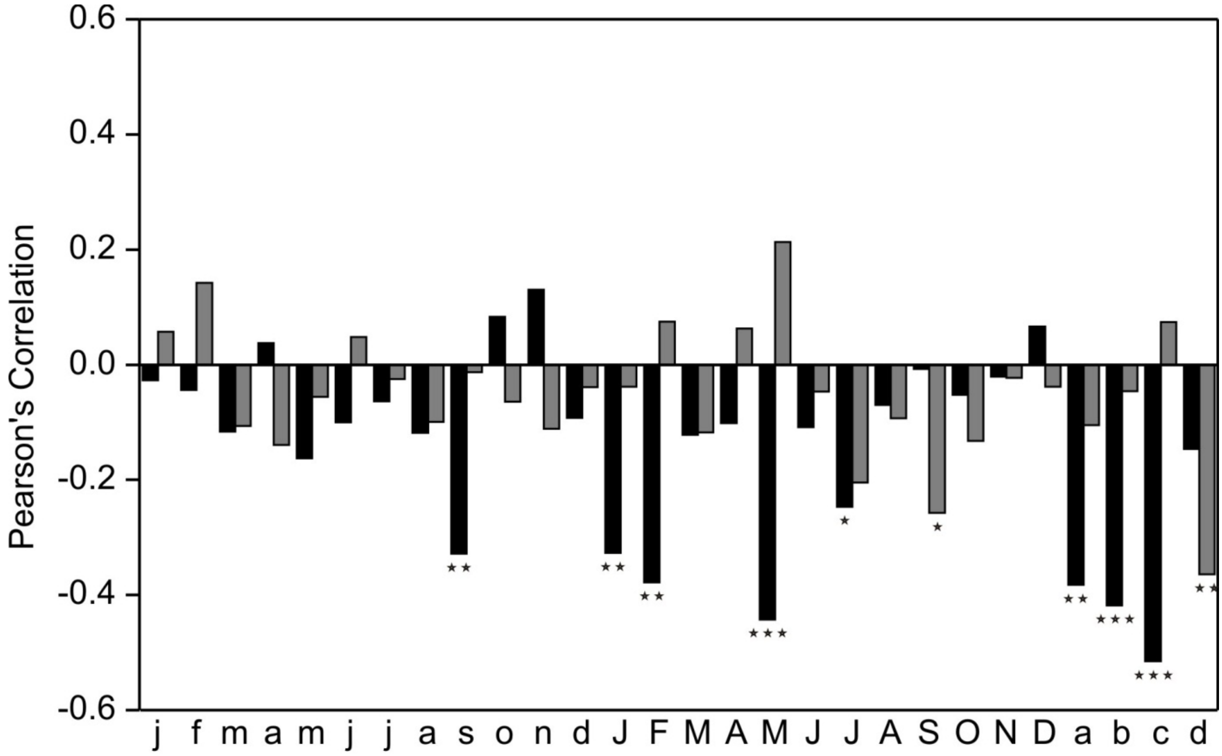

Fig. 3 Climate response plot for the Jsibeli site with the regional climate series (meteorological data from Elmali, Isparta and Afyon): monthly coefficients of correlation for mean temperatures (black bars) and precipitation sums (grey bars), significance levels are 0.05 (*), 0.01 (**), and 0.001 (***). Small letters on the left half of the diagram cover the period January to December of the previous year and capital letters represent January to December of the current year. Small letters a to d stand for annual values (current year) and the periods January-to-March, January-to-May and July-to-September of the current season, respectively.

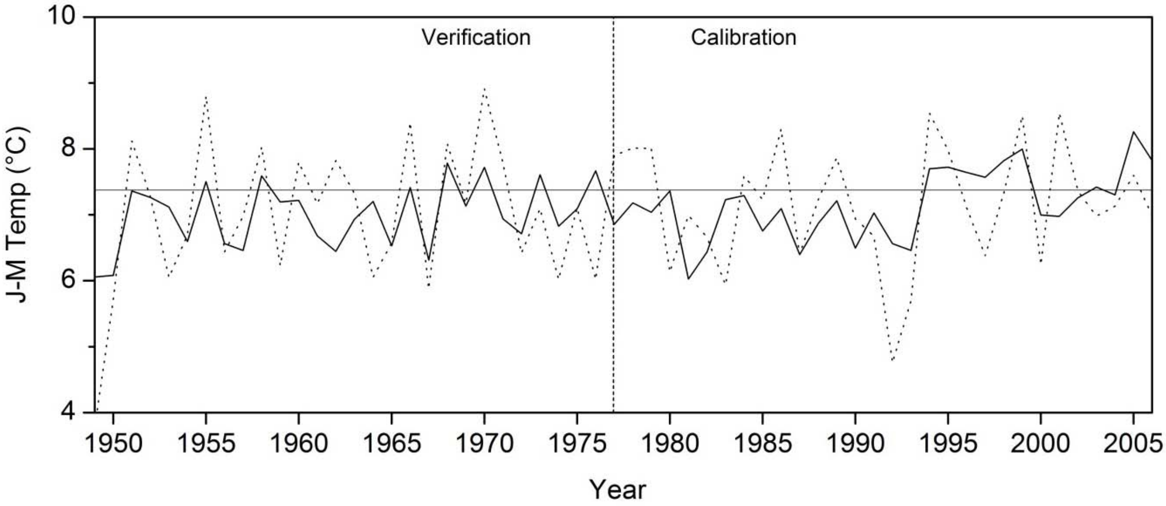

Fig. 4 Reconstructed (solid line) and observed January-to-May temperature (dashed line) for calibration period 1978 to 2006 and verification period 1949 to 1977.

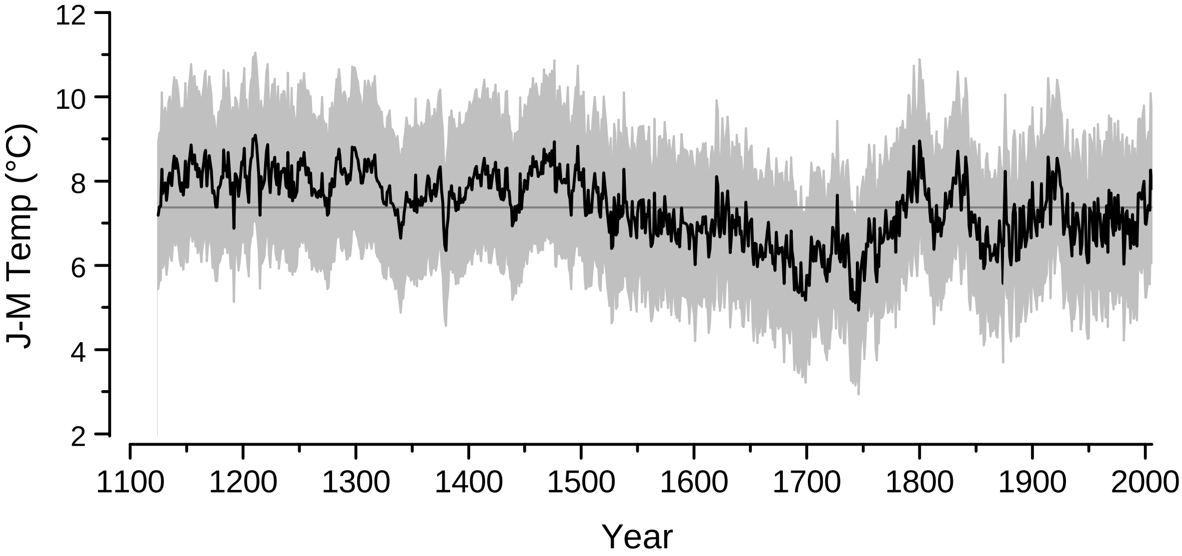

Fig. 5 Reconstruction of January-to-May temperature based on $\delta^{13}C_{CorZ}$ with 95% confidence intervals (CI calculated according to Chou 1972).

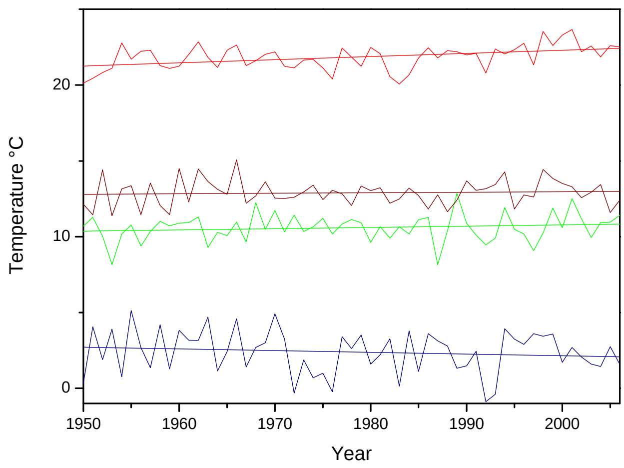

	Coef	SE Coef	t	p
Winter	-1.551	1.559	-1.00	0.324
Spring	2.829	2.457	1.15	0.254
Summer	8.741	2.498	3.50	0.001
Autumn	1.265	2.633	0.48	0.633

Fig. 6 Comparison of trends in seasonal temperature data of composite record Elmali, Isparta and Afyon (Winter: blue, Spring: green, Summer: red, Autumn: brown).

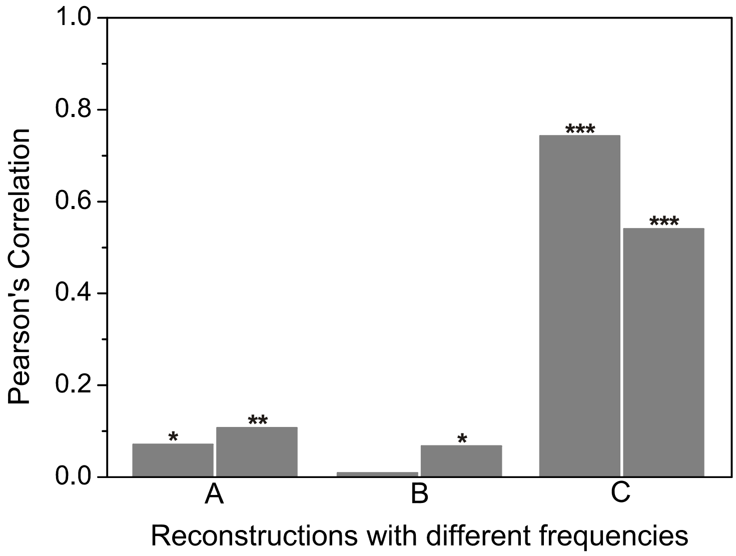

Fig. 7 Correlations (1125-2006) between the Turkish January-to-May temperature reconstruction and two hemispherical temperature reconstructions; high-, band-, and low-pass filtered (A, B, C) versions of Mann et al. 2008 (always left) and Moberg et al. 2005 (always right), significance levels are 0.05 (*), 0.01 (**), and 0.001 (***).

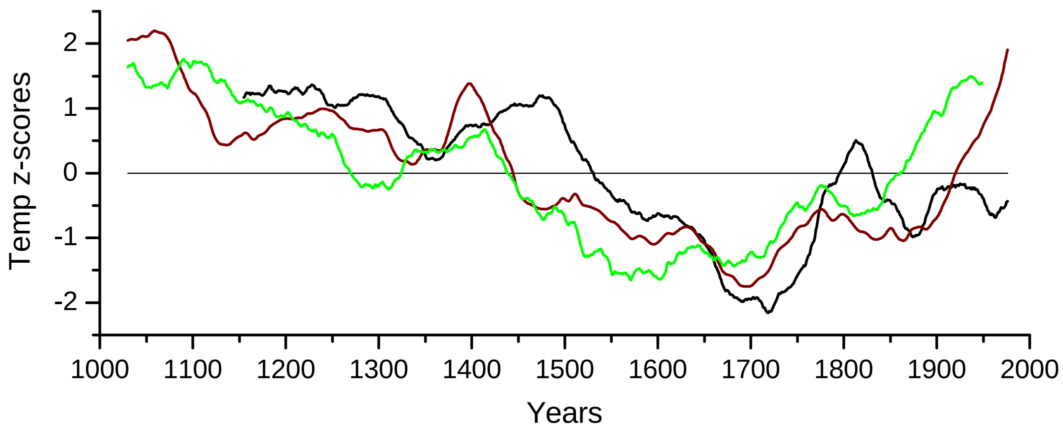

Fig. 8 Comparison of the Turkish January-to-May temperature reconstruction and two hemispherical temperature reconstructions (Mann et al. 2008, brown, and Moberg et al. 2005, green), 61-year moving averages.

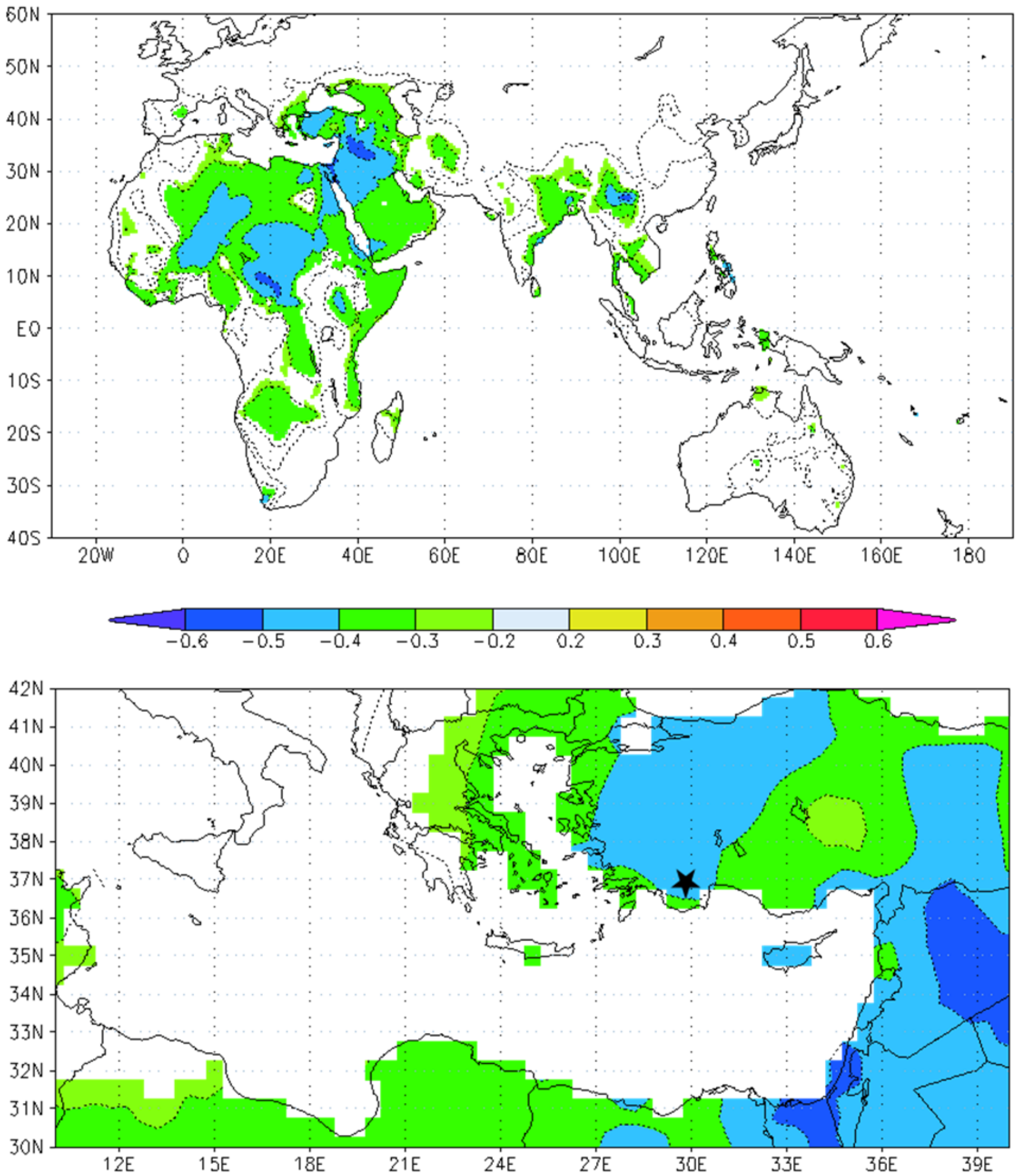

Fig. 9 Spatial field correlations (van Oldenborgh and Burgers, 2005) between mean Jan-May temperature and $\delta^{13}C_{CorZ}$ (1949-2006), upper map: old world overview, lower map: eastern Mediterranean, black star indicates location of the study site.

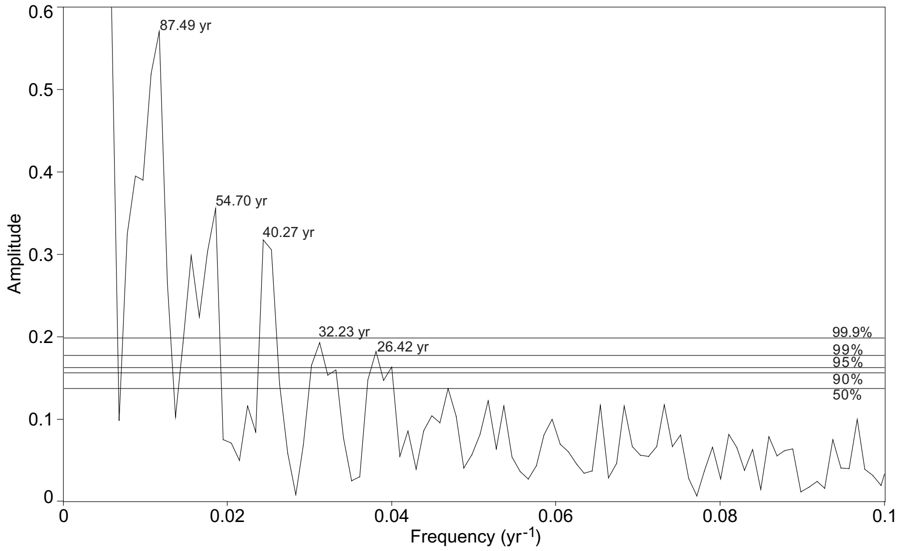

Fig. 10 Spectral analysis of the Jan-May temperature reconstruction for the period 1125-2006 shows significant peaks at approximately 87, 54, 40, 32 and 26 years. 50, 90, 95, 99 and 99.9 % confidence levels are indicated.

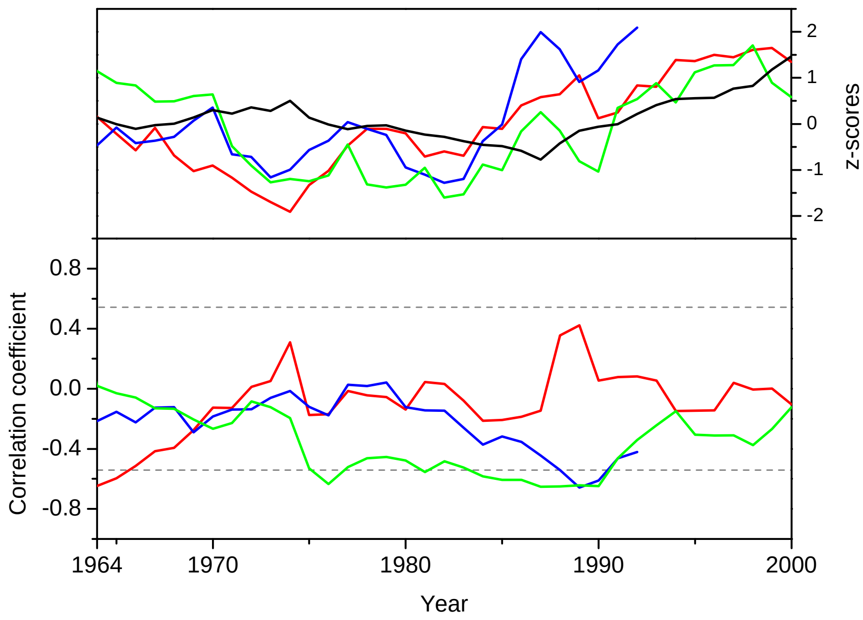

Fig. 11 Coefficients of correlation between Jan-May temperature reconstruction and Jan-May MOI (red), NCPI (blue) and EAWR (green) in moving windows of 13 years (95 % confidence levels are indicated); for comparison printed on top, the z-scores of the corresponding series (MOI red, NCPI blue, EAWR green and Jan-May temperature reconstruction in black, all smoothed with a 13-year mean).

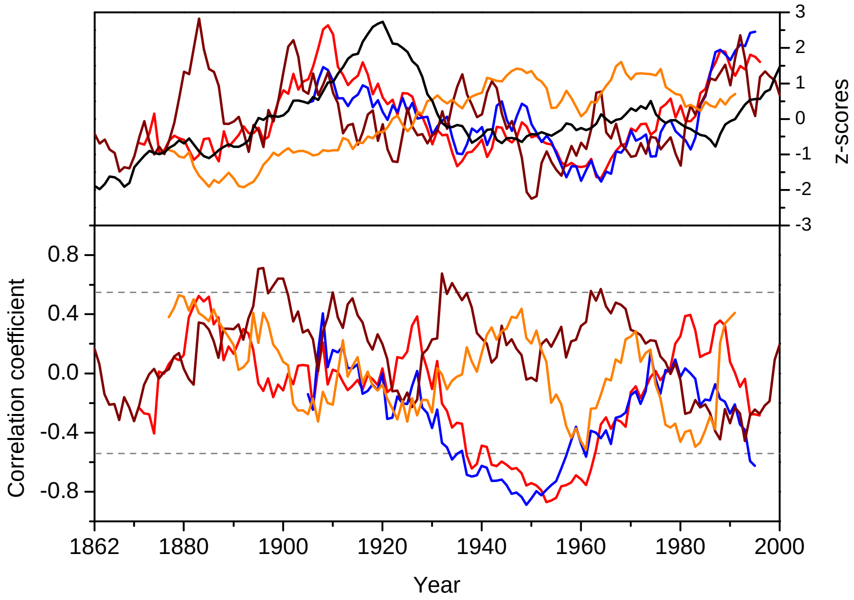

1049

1050 **Fig. 12** Coefficients of correlation between Jan-May temperature reconstruction and Jan-May NAO (red), AO
1051 (blue), NINO4 (brown) and DMI (orange) in moving windows of 13 years (95 % confidence levels are
1052 indicated); for comparison printed on top, the z-scores of the corresponding series (NAO red, AO blue, NINO4
1053 brown, DMI orange and Jan-May temperature reconstruction in black, all smoothed with a 13-year mean).

Table 1 Reconstruction statistics for $\delta^{13}C_{CorZ}$

	$\delta^{13}C_{corZ}$
Full Rsq (2006-1949)	0.27
Rsqcal (2006-1978)	0.18
RsqVer (1977-1949)	0.37
RE	0.29
CE	0.28

Table 2 Comparison of correlations between the Jan-May temperature reconstruction and monthly to seasonal climate indices (NAO, AO, MOI, NCPI, EAWR, NINO4 and DMI) (small letters: months of previous year; capital letters: months of current year; confidence levels: 95%=bolt; 99%=bolt & underlined; 99.9%= bolt, underlined & italics; the confidence intervals differ slightly due to selected time series lengths; 56 yrs: NAO, AO, EAWR, NINO4; 50 yrs: MOI, DMI; 40 yrs: NCPI)

Month/Season	**NAO**	**AO**	**MOI**	**NCPI**	**EAWR**	**NINO4**	**DMI**
jan	0.00	0.04	0.01	-0.07	-0.01	0.18	0.02
feb	0.03	0.05	-0.16	0.04	0.19	0.18	-0.23
mar	0.04	0.11	0.11	0.04	-0.01	0.20	-0.05
apr	0.08	0.19	0.00	-0.11	-0.05	0.23	-0.14
may	**-0.32**	***-0.42***	0.14	**-0.37**	-0.14	**0.28**	0.22
jun	-0.12	-0.22	-0.16	0.01	**0.30**	0.25	**0.28**
jul	0.05	-0.06	0.04	**0.32**	0.00	0.22	0.18
aug	0.21	0.04	**-0.33**	0.13	**-0.33**	0.24	**0.29**
sep	-0.05	-0.04	-0.03	-0.11	-0.16	0.22	0.19
oct	0.04	0.02	-0.02	**0.31**	0.11	0.20	0.11
nov	-0.04	0.05	-0.10	0.04	0.03	0.18	-0.09
dec	0.02	0.07	-0.13	0.09	-0.02	0.17	0.01
Jan	-0.04	-0.13	-0.01	-0.02	-0.18	0.15	0.00
Feb	-0.01	-0.06	-0.10	-0.21	-0.02	0.12	0.16
Mar	0.02	-0.12	-0.07	-0.02	0.02	0.13	-0.02
Apr	-0.22	**-0.36**	0.07	**-0.30**	-0.01	0.09	-0.06
May	0.07	-0.06	-0.05	-0.02	-0.14	0.05	-0.04
apr-may				**-0.36**			
apr-oct						**0.26**	
may-jun	**-0.31**	***-0.42***				**0.28**	**0.28**
may-aug							**0.29**
jun-aug							
jul-oct				**0.27**			
aug-sep					**-0.33**		
Feb-Apr				**-0.27**			
Mar-May		**-0.26**					